Acoustic Feedback Cancellation in Digital Hearing Aids: Tap-Amplitude Based Block Proportionate Adaptive Filtering Approach

A Project Report Submitted

By

Kaushlendra Singh Rathore
(2001EE90)

In Partial Fulfilment
Of the Requirements for the award of the degree

BACHELOR OF TECHNOLOGY

DEPARTMENT OF ELECTRICAL ENGINEERING
INDIAN INSTITUTE OF TECHNOLOGY PATNA
MAY 2024

THESIS CERTIFICATE

This is to certify that the thesis titled **Acoustic Feedback Cancellation in Digital Hearing Aids: Tap-Amplitude Based Block Proportionate Adaptive Filtering Approach,** submitted by Kaushlendra Singh Rathore, to the Indian Institute of Technology, Patna, for the award of the degree of Bachelor of Technology, is a bona fide record of the research work done by him under our supervision. The contents of this thesis, in full or in parts, have not been submitted to any other Institute or University for the award of any degree or diploma.

Somanath Pradhan

Dr. Somanath Pradhan

Supervisor
Assistant Professor
Dept. of Electrical Engineering
IIT-Patna, 801 106

Place: Patna
Date: May 2024

ACKNOWLEDGEMENTS

This research work was supervised by Dr. Somanath Pradhan and was not possible without everyone who has been involved in the work directly or indirectly.

ABSTRACT

Acoustic feedback cancellation has been posing challenges for designing BTE hearing aids. Adaptive filters have been put into usage for the purpose of cancellation of the ill-effects of the same. The feedback path tends to have sparse nature in HA systems. Among the various algorithms being implemented for the purpose of acoustic feedback cancellation, proportionate type algorithms provide better convergence ability for sparse systems. In a move to develop upon the existing algorithms, two new algorithms have been proposed namely PEMABPNLMS-I and PEMABPNLMS-II for HA implementation. The main idea lies behind segmenting similar weights. The first algorithm consists of rearranging the weight vectors to create optimal block partitioning, while the second algorithm utilizes dynamic non-uniform segmentation for the purpose. We further incorporate Prediction Error Method (PEM) with the proposed approach to improve the results. Online input power estimation approach has been integrated for realistic hearing aid implementation. Performance and intelligibility metrices have been monitored for comparative analysis of the effectiveness of the proposed algorithm.

TABLE OF CONTENTS

ACKNOWLEDGEMENTS i
ABSTRACT ii
TABLE OF CONTENTS iii
LIST OF TABLES iv
LIST OF FIGURES v
ABBREVIATIONS vi
ANNOTATIONS vii
INTRODUCTION 1
PROPOSED ALGORITHM 4
Creating Partitions Along x-axis 4
Creating Partitions Along y-axis 6
Acoustic Feedback Cancellation with the Proposed Algorithm 9
STATISTICAL ANALYSIS 11
Bound of Learning Rate 13
Steady State Mean Square Deviation 13
Time Complexity Analysis 14
SIMULATION STUDY 15
Case I: Speech Input Without Path Tracking 16
Case II: Speech Input with Path Tracking 17
Case III: Audio Input with Path Tracking 19
CONCLUSION AND FUTURE SCOPE 23
REFERENCES 24

LIST OF TABLES

Table 1 : Summary of PEM-ABPNLMS - I 7

Table 2: Summary of proposed PEM_ABPNLMS-II..... 8

Table 3: Comparison of Computational Complexity per Iteration 14

Table 4: PESQ and HASQI Score for Speech signal without path tracking. 17

Table 5: PESQ Score for observed change in acoustic path - Path Tracking in case of speech input 18

Table 6: HASQI Score for observed change in acoustic path for speech input..... 18

Table 7: PEAQ Score for observed change in acoustic path - Path Tracking in case of speech input 19

Table 8 : HAAQI Score for observed change in acoustic path..... 19

LIST OF FIGURES

Figure 1. Example showcasing (a) block divisions along x-axis (b) assigning partitions after rearranging weight vectors along x-axis with P = 20 (b) y-axis based divisions using variable ζ . 4

Figure 2: Schematic Block Diagram of a common Acoustic Feedback Cancellation System with Gain Gz, the acoustic feedback path Fz, The estimated Feeback Path Fz, the loudspeaker signal v(n), the microphone signal u(n) and the error signal e(n). 10

Figure 3: Power Spectral Density of the Acoustic Feedback paths 16

Figure 4:(a) Speech input signal and corresponding (b) MIS (c) ASG (d) MSG plots for acoustic feedback cancellation in Hearing aids 20

Figure 5(a) Speech input signal and corresponding (b) MIS (c) ASG (d) MSG plots for acoustic feedback cancellation in Hearing aids for path tracking..... 21

Figure 6(a) Audio input signal and corresponding (b) MIS (c) ASG (d) MSG plots for acoustic feedback cancellation in Hearing aids for path tracking..... 22

ABBREVIATIONS

AFC	Acoustic Feedback Cancellation
ASG	Added Stable Gain
BS-PNLMS	Block Sparse Proportionate Normalized Least Mean
BTE	Behind The Ear
BZA-LMS	Block Zero Attraction Least Mean Square
FIR	Finite Impulse Response
HA	Hearing Aid
HAAQI	Hearing Aid Audio Quality Index
HASQI	Hearing Aids Speech Quality Index
IPNLMS	Improved Proportionate Normalized Least Mean Square
LMS	Least Mean Square
MIS	Misalignment
MSD	Mean Square Deviation
MSG	Maximum Stable Gain
NLMS	Normalized Least Mean Square
PAS	Public Address System
PEAQ	Perceptual Evaluation of Audio Quality
PEM	Prediction Error Method
PESQ	Perceptual Evaluation of Speech Quality
VSS	Variable Step Size
ZA-LMS	Zero-Attraction Least Mean Square

ANNOTATIONS

$\mathbb{E}[\cdot]$	Expectation
$\boldsymbol{P}$	Proportionate Matrix
$\boldsymbol{I}_L$	Identity Matrix
$\boldsymbol{X}_p$	Prefiltered signal
$\boldsymbol{R}_{\boldsymbol{uu}}$	Autocorrelation matrix of signal $\boldsymbol{u}$
$\boldsymbol{r}_{eu}$	Correlation between e and $\boldsymbol{u}$
$\hat{\sigma}_x^2$	Signal Power
$\boldsymbol{x}^{\boldsymbol{H}}$	Hermitian matrix

CHAPTER 1

INTRODUCTION

A frequently encountered challenge in closed-loop systems such as public address system (PAS) and open-fit hearing aid (HA) is the occurrence of acoustic feedback due to the close proximity of loudspeaker and microphone. The presence of acoustic feedback not only degrades the desired signal quality, but also imposes limitations on the maximum stable gain that can be achievable. Under specific conditions, it can lead to system instability [1][2], potentially giving rise to occurrence of howling when the loop gain exceeds one at a frequency where the loop phase aligns with multiples of 2π. One obvious solution might be the complete shielding of loudspeaker sound from the microphone sound by means of an earmuff. However, it results in occlusion effect due to the trapping of bone conducted sound when the outer ear is occluded. The forward path gain reduction technique and vent in hearing aid are not effective for hearing aid users. [3]

Adaptive feedback cancellation scheme based on the deployment of adaptive digital filters has gained momentum in recent years. The adaptive filter is likely to address the variation of acoustic feedback path due to changes in the acoustic environment around the hearing aid such as head movement, use of mobile phones, traveling in a vehicle, chewing food, thermal fluctuations, room reverberation and changing sitting position. The acoustic feedback canceller is a finite impulse response (FIR) filter which models the acoustic feedback path from loudspeaker to the microphone using some adaptive algorithm, generates an estimation of feedback signal and cancels the feedback signal internally. The feedback compensated signal is then fed to the forward path gain. In a conventional digital hearing aid, the least mean square (LMS) or normalized LMS

(NLMS) algorithm is deployed for feedback cancellation. However, the algorithm is prone to slow convergence due to highly correlated input signals [4] such as speech and music. Furthermore, the finite correlation between the input and output signals of the hearing aid leads to a biased estimation of acoustic feedback path which in turn cancels the desired signal along with the feedback signal resulting in a distortion in desired signal. [5]

Numerous means have been proposed to minimize the bias associated with the feedback path estimation which includes inserting delay in forward path [6], [7], frequency shifting [8], [9], phase shifting in forward path and adding a probe signal to the loudspeaker input [10],[11] and constrained or bandlimited adaptation. However, these techniques possess a tradeoff between biased estimation of feedback path and output sound quality [5]. Prediction error method (PEM) is one of the promising methods to reduce the bias in the estimation process in which the feedback compensated signal and the input signal to loudspeaker are pre filtered by the prediction error filter before being fed to the feedback cancellation algorithm. Several adaptive feedback cancellation algorithms integrated with PEM technique have been reported [12][13][14][15][16][17]. A robust technique for minimizing effects of impulsive noise is introduced in [18].

The acoustic feedback paths of hearing aids are typically sparse in nature as a large number of coefficients in the impulse response are zeros or close to zeros. Sparsity-aware adaptive filters as the feedback canceller can significantly improve the convergence behavior. Several feedback cancellation mechanisms have been proposed integrating the PEM technique and sparsity-aware adaptive filters. A sparsity-aware adaptive feedback cancellation mechanism has been developed based on the principle of zero attraction [19]. Moreover, [20] provides a study over the use of two microphones and one loudspeaker in AFC. Another algorithm using two adaptive filters, each for input signal and probe signal respectively, has been discussed in [21].

Several algorithms discussing the aforementioned issues have been proposed where we see many general sparse approaches including zero-attraction type algorithms such as ZA-LMS [22] and versions of $\ell 0$-LMS as developed in [23] and [24] among others. Other approaches considered block-sparsity to develop, for example, BZA-LMS [25] and improvised versions such as $l_{2,0}$-BS-PNLMS [26]. These algorithms suffer from improper block segmentation which leads to uneven blocks containing zero and significant non-zero taps. This undermines our intent to assign the same proportional gain to each block based on their weights.

In this paper, two new algorithms are developed for acoustic feedback cancellation in hearing aid integrating PEM technique and block proportionate technique with the tap-amplitude-based block partitioning. In the first algorithm, the weight vectors are rearranged to create blocks of uniform division by performing sorting operations, which comprises of similar sized weights. The sorting operation is carried out on the x-axis and the proportional gain depends on the partitioning of the x-axis. It is worth noting that these divisions on x-axis are performed such that each block comprises of the same number of tap-weights. The second algorithm involves assigning proportional gain by dynamic non-uniform partitioning of the y-axis. The PEM method aims at reducing the bias associated with the feedback path estimation process whereas the two novel block proportionate techniques aid in achieving improved performance.

The remainder of the article is organized as follows. Section II presents the overview of the proposed algorithm for acoustic feedback cancellation. The convergence analysis and computational complexity is studied in Section III. Simulation study is carried out in Section IV and concluding remarks are made in Section V.

CHAPTER 2

PROPOSED ALGORITHM

We have discussed the proposed algorithms in the following section, of which the algorithm wherein we utilize partitioning along the x-axis will termed as PEM-ABPNLMS-I and similarly, the algorithm assigning partition along the y-axis is termed as PEM-ABAPNLMS-II here onwards.

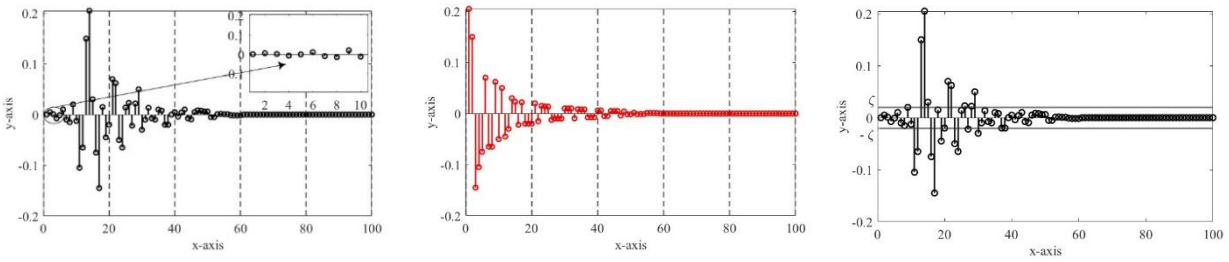

Figure 1. Example showcasing (a) block divisions along x-axis (b) assigning partitions after rearranging weight vectors along x-axis with P = 20 (b) y-axis based divisions using variable ζ

Creating Partitions Along x-axis

We tend to create blocks along the x-axis, which contain similar sized weight vectors. The weight vector $f(i)$ is rearranged in descending order of magnitude values by performing sorting operation. This gives us

$$\boldsymbol{f}_S(i) \;=\; [f_{(1)}^{m}(i), f_{(2)}^{k}(i), \dots, f_{(L)}^{h}(i)]^T \qquad (1)$$

with $\left|f_{(1)}^{m}(i)\right| \geq \left|f_{(2)}^{k}(i)\right| \geq \cdots \geq \left|f_{(L)}^{h}(i)\right|$. In the equation (1), the subscript is the descending order rearranged while the superscript denotes the original position in the weight vector f. We use the $l_{2,1}$- norm of $f_s(i)$.

$$\|f_s(i)\|_{2,1} = \sum_{m=1}^{M} \left\|f_{[m]}(i)\right\|_2 \qquad (2)$$

where the m-th division of the block within $f_s(i)$ is represented by $f_{[m]}(i)$. The sorted weight

vectors, then can be used to derive regularized mean-square estimation.

$$min\ \mathbb{E}\{(d(i) - u_s{}^T f_s)^2\} + \rho\|\boldsymbol{Q}^{-1} f_s\|_{2,1} \quad (3)$$

with ρ being used for regularization and the term $\boldsymbol{Q}^{-1} f_s$ becomes block sparse. We thus iteratively calculate

$$\min_{\boldsymbol{h}_s} \mathbb{E}\{(d(i) - u_s{}^T \boldsymbol{Q} h_s)^2\} + \rho G(h_s) \quad (4)$$

Where $G(\mathbf{h_s}) = \sum_{l=1}^{M} \left\| h_{([l])} \right\|_2$ is block sparse regulation term and $\boldsymbol{h_s} = [\boldsymbol{h}_{([1])}^T, \dots, \boldsymbol{h}_{([M])}^T]^{\boldsymbol{T}}$. We use LMS scheme, to get the recursive solution.

$$h_s(i+1|i) = h_s(i) + \mu'(\boldsymbol{Q} u_s(i) e(i) - \rho \Phi(i) \boldsymbol{h}_s(i) \quad (5)$$

where

$$\Phi(i) = diag\left(\left[\frac{1}{\|h_{([1])}(i)\|_2} \mathbb{I}_P, \dots, \frac{1}{\|h_{([M])}(i)\|_2} \mathbb{I}_P\right]\right) \quad (6)$$

and $\mathrm{h}_s(i) = \left[\mathrm{h}_{([1])}{}^T(i), .., \mathrm{h}_{([M])}{}^T(i)\right]^T$. Solving for μ' , we arrive at

$$\mu' = \mu \frac{1}{\boldsymbol{u}_s^T(i) \boldsymbol{Q^2} u_s(i)} \quad (7)$$

We can then write.

$$f_s(i+1|i) = f_s(i) + \mu \frac{\boldsymbol{Q^2} u_s(i) e(i) - \rho \Phi(i) f_s(i)}{\boldsymbol{u}_s{}^T \boldsymbol{Q^2}(i) \boldsymbol{u}_s(i)} \quad (8)$$

Putting $\rho = 0$ for above equation and replacing $\boldsymbol{Q^2}$ with $\boldsymbol{P_s} = \boldsymbol{Q^2}/\boldsymbol{Tr}(\boldsymbol{Q^2})$ which is the normalized representation of it. We thus update the weight vector as follows:

$$f_s(i+1|i) = f_s(i) + \mu \frac{\boldsymbol{P}_s(i) \boldsymbol{u}_s(i)}{\mathbf{u}_s{}^T \boldsymbol{P}_s(i) \boldsymbol{u}_s(i) + \epsilon} e(i) \quad (9)$$

Where the entries of $u_s(i)$ are rearranged in accordance with the reshuffling of $f(i)$ to arrive at $f_s(i)$. Furthermore, we define $e(i) = d(i) - u_s{}^T f_s(i)$, and

$$\boldsymbol{P}_s(i) = diag\{p_{[1]}(i), p_{[2]}(i), \dots, p_{[M]}(i)\} \otimes \boldsymbol{I}_P \quad (10)$$

with

$$p_{[m]}(i) = \frac{1-\gamma}{2L} + \frac{(1+\gamma)\left\| f_{([m])}(i)\right\|_2}{2P\sum_{m=1}^{M}\left\|f_{([m])}(i)\right\|_2+\epsilon} \quad (11)$$

According to the definition of $\boldsymbol{f}_s(i)$, the equation (2) providing us $\boldsymbol{f}_s(i+1|i)$, aligns with the order of $\boldsymbol{f}_s(i)$ and therefore can give divergence from $\boldsymbol{f}_s(i+1)$. To ensure a continuous updating process, we apply a sorting operation to the outcome of equation (2) to derive $\boldsymbol{f}_s(i+1)$ at time $i+1$.

By adhering to the original arrangement of the taps, the utilization of equation (2) leads to the equivalent rearrangement and updating of the original weights.

$$\mathbf{f}(i+1) = \mathbf{f}(i) + \mu\frac{\boldsymbol{P'}(i)\boldsymbol{u}(i)}{\boldsymbol{u}^T\boldsymbol{P'}(i)\boldsymbol{u}(i)+\epsilon}e(i) \quad (12)$$

where $\boldsymbol{P'}(i) = diag\{p'_1(i), p'_2(i), \dots, p'_L(i)\}$. After rearranging the weight vectors if $f_m(i)$ is housed in the block $f_{([l])}(i)$, then we put $p'_m(i) = p_{[l]}(i)$.

Creating Partitions Along y-axis

Subsequently, we now look for a non-uniform partitioning approach along the y-axis. To streamline the process, we categorize all tap weights into two distinct groups, denoted as $N_1(i)$ and $N_2(i)$, based on a designated threshold value, ζ, and the respective magnitudes of the weights. In other words, we classify the weights into these two groups according to their magnitude relative to the threshold ζ.

$$|f_l(i)| \leq \zeta, l \in N_1(i) \quad (13)$$

$$|f_l(i)| > \zeta, l \in N_2(i) \quad (14)$$

Given that the sizes of $N_1(i)$ and $N_2(i)$ may vary, we compute the proportional gain by averaging-out the tap amplitudes within the designated intervals.

$$p_l(i) = \begin{cases} \frac{1-\gamma}{2L} + \frac{(1+\gamma)a_1(i)}{2\left(|N_1(i)|a_i(i)+|N_2(i)|a_2(i)\right)+\epsilon}, & l \in N_1(i) \\ \frac{1-\gamma}{2L} + \frac{(1+\gamma)a_2(i)}{2\left(|N_1(i)|a_i(i)+|N_2(i)|a_2(i)\right)+\epsilon}, & l \in N_2(i) \end{cases} \quad (15)$$

where we use the terms $a_1(i) = \frac{1}{|N_1(i)|}\sum_{l \in N_1(i)}|f_l(i)|$ and $a_2(i) = \frac{1}{|N_2(i)|}\sum_{l \in N_2(i)}|f_l(i)|$. We have already discussed the decreased convergence rates when algorithm is nearing steady states. To shed light on the issue we use a time varying threshold:

$$\zeta = \kappa\lambda(i)\frac{||f(i)||_1}{L} \qquad (16)$$

where κ represents a tunable hyper-parameter[1] in the range (0, 1]. Highlighting the time varying term $\lambda(i)$ is expected to be close to 1 in transient state and close to 0 in near convergence. We update the term $\lambda(i)$ using the following equation:

$$\lambda(i) = \begin{cases} \frac{\hat{\sigma}_e^2(i) - \hat{\sigma}_x^2(i)}{\hat{\sigma}_e^2(i) + \epsilon}, & if\ \hat{\sigma}_e^2(i) > \hat{\sigma}_x^2(i) \\ 0 & otherwise \end{cases} \qquad (17)$$

The value of $\hat{\sigma}_e^2(i)$ is calculated iteratively using the equation $\hat{\sigma}_e^2(i) = \beta\hat{\sigma}_e^2(i-1) + (1-\beta)e_p^2(i)$ with an initialization with $\hat{\sigma}_e^2(i) = 0$ and $0 \ll \beta < 1$. The estimations for $\hat{\sigma}_x^2(i)$ specific to acoustic feedback cancellation, have been discussed separately in the following sub-section.

Table 1 : Summary of PEM-ABPNLMS - I

Initialization: $f_l(0) = 0, \epsilon, \gamma, \mu, P, L, M$

For i = 1,2,3…
Calculate $p_l(i)$:
$\boldsymbol{f}(i) = [|f_1(i)|, |f_2(i)|, \dots, |f_L(i)|]^T$;
[$\boldsymbol{f}_s(i)$, c] = sort($f(i)$,"descend","ComparisonMethod","abs") ;
%Rearranging the weight vector in descending order
%$\boldsymbol{f}_s(i)$ contains the sorted weight vectors data and
% $\boldsymbol{c}$ array has the corresponding indices of $\boldsymbol{f}(i)$

g = zeros(L,1); s = 0;
for m = 1:M
  for $j = (m-1)P + 1 : mP$
    $temp(j - (m-1)P) = \boldsymbol{f}(j)$;
  end
    $\delta = \|\text{temp}\|_2$

[1] When κ is approximately equal to zero, the PEM-ABPNLMS-II algorithm will transition into the NLMS, which leads to a slower starting convergent rate. We recorded that κ values ranging from 0.2 to 0.5 are effective for block-sparse systems, while κ values between 0.8 and 1 perform well for general sparse systems.

for $ii = (m-1)P+1 : mP$
$g(c(ii)) = del;$
end
$s = s + \delta;$
end
$p = \frac{1-\gamma}{2L} + \frac{(1+\gamma)g}{2sP+\epsilon};$
$\boldsymbol{P}'(i)$ = diag{p};

Weight update step:
$e(i) = d(i) - \mathbf{u}^T(i)\boldsymbol{f}(i);$
PEM filter step:
$e_p(i) = \boldsymbol{e}(i) * \boldsymbol{f}_p(i);$
use equation (3);
end

Table 2: Summary of proposed PEM_ABPNLMS-II

Initialization: $\hat{\sigma}_e^2(0)=0, \hat{\sigma}_x^2(0)=0, f_l(0)=0, \epsilon, \gamma, \mu, \kappa, \beta$

For i = 1,2, …
$e(i) = d(i) - \boldsymbol{u}^T(i)\boldsymbol{f}(i);$
PEM filter step:
$\mathbf{e_p}(i) = \boldsymbol{e}(i) * \boldsymbol{f}_p(i);$
$\boldsymbol{u_p}(i) = \boldsymbol{u}(i) * \boldsymbol{f}_p(i);$
Noise power update equation:
$\sigma_{\mathbf{e}}^2(i) = \beta\hat{\sigma}_e^2(i-1) + (1-\beta)\boldsymbol{e_p^2}(i)$
$\sigma_{\mathbf{u}}^2(i) = \beta\sigma_{\mathbf{u}}^2(i-1) + (1-\beta)\,\mathbf{u_p^2}(i)$
Recursively update Noise correlation matrix:
$\boldsymbol{r}_{eu} = \beta.\boldsymbol{r}_{eu} + ((1-\beta)\boldsymbol{e}(i).\mathbf{u}(i)$
$\boldsymbol{R_{uu}} = \beta.\boldsymbol{R_{uu}} + ((1-\beta)\mathbf{u}(n).\mathbf{u}^H(i)$
$\boldsymbol{R_{ee}} = \beta.R_{ee} + ((1-\beta).\boldsymbol{e}(n).\boldsymbol{e}^H(i)$
$\tilde{R}_{uu} = \frac{1}{2}(R_{uu}(n) + \boldsymbol{R_{ee}}(n)(\sigma_u^2(n)/\sigma_e^2(n)))$
$\hat{\sigma}_x^2(n) = \hat{\sigma}_e^2(n) + \boldsymbol{r}_{\boldsymbol{eu}}^H(n)\left(\boldsymbol{R_{uu}^{-1}}(n)\right)^H \boldsymbol{r_{eu}}(n) - 2.\mathrm{Re}\left\{\left(\boldsymbol{r}_{\boldsymbol{eu}}^H(\mathrm{n})\left(\boldsymbol{R_{uu}^{-1}}(n)\right)^H \boldsymbol{r_{eu}}\right)\right\};$
$\lambda = \left(\sigma_e^2(i) - \sigma_x^2(i)\right)/\sigma_e^2(i) + \epsilon$
$\zeta = \kappa\lambda(i)\left|\left|\boldsymbol{f}(i)\right|\right|_1/L$
$a1 = 0;$
$V = 0;$
for l = 1: L
if $(abs(h\_hat(l)) <= \zeta)$
a1=a1+$abs(h\_hat(l))$;
$V = V + 1;$
end
end
$g_1 = (1-\gamma)/(2*L) + (1+\gamma)*a_1/((N)*(2*norm(h\_hat,1) + \epsilon));$

$g_2 = (1 - g1 * V)/(L - V)$;

for l = 1: L
  if (V==0)
    $p(l) = 1/L$;
  elseif (abs(h_hat(l)) <= ζ)
    $p(l) = g_1$;
  else
    $p(l) = g_2$;
  end
end
$\boldsymbol{P} =$ diag(p);
Weight update equation:
Equation (12)
end

Acoustic Feedback Cancellation with the Proposed Algorithm

The value for input signal power $\hat{\sigma}_x^2(i)$ is estimated using the equation:

$$\hat{\sigma}_x^2(n) = \hat{\sigma}_e^2(n) + \boldsymbol{r}_{eu}^H(n)\left(\boldsymbol{R}_{\boldsymbol{uu}}^{-\mathbf{1}}(n)\right)^H r_{eu}(n) - 2.Re\left\{\left(\boldsymbol{r}_{eu}^H(n)\left(\boldsymbol{R}_{\boldsymbol{uu}}^{-\mathbf{1}}(n)\right)^H \boldsymbol{r}_{\boldsymbol{eu}}\right)\right\} \quad (18)$$

where R_{uu} is the autocorrelation matrix for loudspeaker output signal and r_{eu} is the cross-correlation vector between error signal and loudspeaker output. We compute both the terms using the following equation:

$$\boldsymbol{r}_{\boldsymbol{eu}} = \beta.\boldsymbol{r}_{\boldsymbol{eu}} + ((1-\beta)\boldsymbol{e}(i).\boldsymbol{u}(i) \quad (19)$$

$$\boldsymbol{R}_{\boldsymbol{uu}} = \beta.\boldsymbol{R}_{\boldsymbol{uu}} + ((1-\beta)\boldsymbol{u}(n).\boldsymbol{u}^H(i) \quad (20)$$

A modified estimation of the autocorrelation matrix is developed in [27]. We thus replace R_{uu} with

$$\widetilde{\boldsymbol{R}}_{\boldsymbol{uu}} = \frac{1}{2}\left(\boldsymbol{R}_{\boldsymbol{uu}}(n) + \boldsymbol{R}_{\boldsymbol{ee}}(n)\frac{\sigma_u^2(n)}{\sigma_e^2(n)}\right) \quad (21)$$

where

$$\boldsymbol{R}_{\boldsymbol{ee}} = \beta.\boldsymbol{R}_{\boldsymbol{ee}} + ((1-\beta).\boldsymbol{e}(n).\boldsymbol{e}^{\boldsymbol{H}}(i) \quad (22)$$

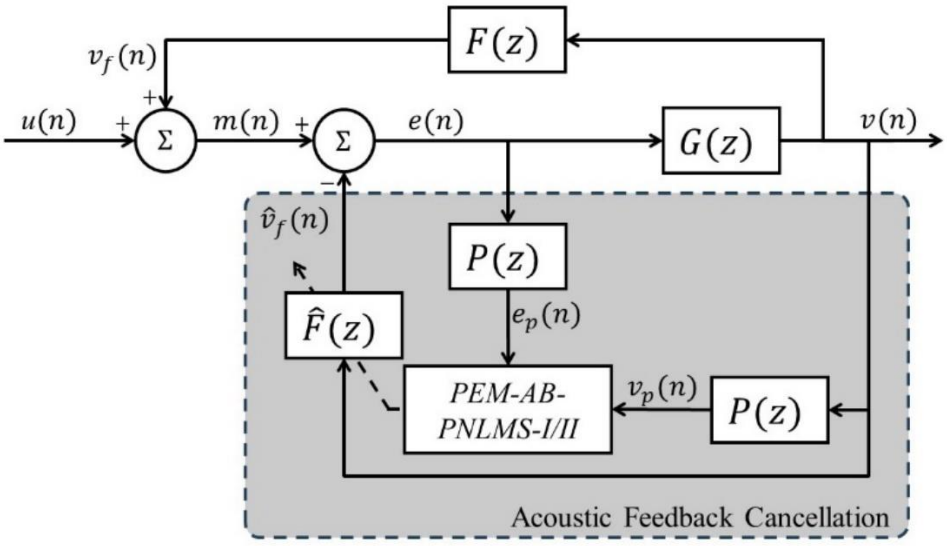

Figure 2: Schematic Block Diagram of a common Acoustic Feedback Cancellation System with Gain G(z), the acoustic feedback path F(z), The estimated Feeback Path $\hat{F}(z)$, the loudspeaker signal v(n), the microphone signal *u*(n) and the error signal *e*(n).

Due to the presence of a high correlation between the microphone signal and loudspeaker output, the cancellation schemes don't work effectively. The feedback cancellation system tends to cancel out more of the microphone signal than the feedback output, decreasing the system performance significantly. Therefore, to improve the performance of the system, we have used the Prediction Error Method to de-correlate the signals.

The main contributions of this work can be summarized in the following points:

- Development of the two algorithms namely PEMABPNLMS-I and PEMABPNLMS-II for acoustic feedback cancellation in hearing aids.
- Applying effective input power estimation technique for online estimations of input power for practical use cases.
- Integration of Prediction Error Method with the algorithms to further improve the performance of the algorithms using Levinson- Durbin algorithm.

CHAPTER 3

STATISTICAL ANALYSIS

For the PEMABPNLMS-I algorithm, computing the expectation of P′(i) is complicated because of sorting operations. Thus, in this section, we only carry out the statistical analysis of PEMABPNLMS-II. In general, the mean and mean-square analysis of proportional-type algorithms is challenging, due to the magnitude of the weight entries, which determine the proportional matrices. To facilitate the convergence analysis, we introduce three customary assumptions.

We have used PEM filter for decorrelating the error and loudspeaker signals, given by

$$\mathrm{e}_p(i) = \mathbf{e}(\mathrm{i}) * \boldsymbol{f}_p(\mathrm{i}) \quad (23)$$

and u_p

$$u_p(i) = \boldsymbol{u}(\mathrm{i}) * \boldsymbol{f}_p(\mathrm{i}) \quad (24)$$

For the ease of transient and steady state analysis, we introduce a few sets of assumptions which are generally implemented for the use cases.

Assumption (i):

We take a valid assumption that the input signal $\{\underline{\boldsymbol{u}_{\mathrm{p}}(i)}\}$ independent, zero-mean, and stationary white Gaussian random sequences with a variance of $\sigma^2_{\boldsymbol{u}_p}(i)$.

Assumption (ii):

We represent the noise signal as $\{\mathbf{v}_{\mathrm{p}}(\mathrm{i})\}$, and considering it to be independent, having a mean of 0, and the signal to be stationary random variables. We denote the variance of the noise as $\sigma^2_{\mathbf{v}_{\mathrm{p}}}(\mathrm{i})$, where $\mathbb{E}\{\mathbf{v}_{\mathrm{p}}{}^2(\mathrm{i})\}$ represents the expected value of the square of the signal $\mathbf{v}_{\mathrm{p}}(\mathrm{i})$. Additionally, these noise signals are statistically independent of the sequence $\{\boldsymbol{u}_{\mathrm{p}}(\mathrm{i})\}$.

Assumption (iii):

The sequence $w(i)$ is statistically independent of $u_p(i)$. This assumption of independence is widely recognized and frequently employed in the analysis of adaptive filters.

We denote the weight error vector $\tilde{\boldsymbol{f}}(i) = \boldsymbol{f}_{opt} - \boldsymbol{f}(i)$. From (12), we have the recursive formulas for $\tilde{f}(i)$ and $\tilde{f}(i)\tilde{f}^T(i)$:

$$\tilde{f}(i+1) = \tilde{f}(i) - \mu \frac{P(i)\boldsymbol{u}_p(i)\boldsymbol{u}_p{}^T(i)}{\boldsymbol{u}_p{}^T(i)P(i)\boldsymbol{u}_p(i)}\tilde{f}(i) - \mu \frac{P(i)\boldsymbol{u}_p(i)}{\boldsymbol{u}_p{}^T(i)P(i)\boldsymbol{u}_p(i)}\mathbf{v}_p(i) \qquad (25)$$

And

$$\tilde{\boldsymbol{f}}(i+1)\tilde{\boldsymbol{f}}^T(i+1) = \tilde{\boldsymbol{f}}(i)\tilde{\boldsymbol{f}}^T(i) - \mu \frac{\boldsymbol{P}(i)\boldsymbol{u}_p(i)\boldsymbol{u}_p{}^T(i)\tilde{\boldsymbol{f}}(i)\tilde{\boldsymbol{f}}^T(i)}{\boldsymbol{u}_p{}^T(i)\boldsymbol{P}(i)\mathbf{u}_p(i)} - \mu \frac{\tilde{\boldsymbol{f}}(i)\tilde{\boldsymbol{f}}^T(i)\boldsymbol{u}_p(i)\boldsymbol{u}_p{}^T(i)\mathbf{P}(i)}{\boldsymbol{u}_p{}^T(i)\boldsymbol{P}(i)\boldsymbol{u}_p(i)}$$

$$+\mu^2 \frac{\mathbf{P}(i)\boldsymbol{u}_p(i)\boldsymbol{u}_p{}^T(i)\tilde{\boldsymbol{f}}(i)\tilde{\boldsymbol{f}}^T(i)\boldsymbol{u}_\mathbf{p}(i)\boldsymbol{u}_\mathbf{p}{}^T(i)\mathbf{P}(i)}{\left(\boldsymbol{u}_\mathbf{p}{}^T(i)\mathbf{P}(i)\boldsymbol{u}_p(i)\right)^2}$$

$$+\mu^2 \boldsymbol{v}_\mathbf{p}{}^2(i) \frac{\mathbf{P}(i)\boldsymbol{u}_p(i)\boldsymbol{u}_\mathbf{p}{}^T(i)\boldsymbol{P}(i)}{\left(\boldsymbol{u}_p{}^T(i)\mathbf{P}(i)\boldsymbol{u}_\mathrm{p}(i)\right)^2} \qquad (26)$$

Using the appropriate substitute for $\mathbf{u}_\mathrm{p}{}^T(\mathrm{i})\mathbf{P}(\mathrm{i})\mathbf{u}_\mathbf{p}(\mathrm{i}) = \sigma^2_{\boldsymbol{u}_\mathrm{p}}$ for the usage of long adaptive filters as in [28] and finding the expectation of the above equations under our assumptions

$$\mathbb{E}\{\tilde{\boldsymbol{f}}(i+1)\} \approx \mathbb{E}\{\tilde{\boldsymbol{f}}(i)\} - \mu\mathbb{E}\{\boldsymbol{P}(i)\tilde{\boldsymbol{f}}(i)\} \qquad (27)$$

And

$$\mathbb{E}\{\tilde{\boldsymbol{f}}(i+1)\tilde{\boldsymbol{f}}^T(i+1)\} \approx \mathbb{E}\{\tilde{\boldsymbol{f}}(i)\tilde{\boldsymbol{f}}^T(i)\} - \mu\mathbb{E}\{\mathbf{P}(i)\tilde{\boldsymbol{f}}(i)\tilde{\boldsymbol{f}}^T(i)\}$$

$$-\mu\mathbb{E}\{\tilde{\boldsymbol{f}}(i)\tilde{\boldsymbol{f}}^T(i)\mathbf{P}(i)\} + \frac{\mu^2}{\sigma^4_{\mathbf{u}_\mathbf{p}}}\mathbb{E}\{\mathbf{P}(i)\mathbf{u}_p(i)\mathbf{u}_\mathrm{p}{}^T(i)\tilde{\boldsymbol{f}}(i)\tilde{\boldsymbol{f}}^T(i)\mathbf{u}_p(i)\mathbf{u}_p{}^T(i)\mathbf{P}(i)\}$$

$$+\mu^2 \sigma^2_{\mathbf{v}_p}\mathbb{E}\{\mathbf{P}^2(i)\} \qquad (28)$$

Applying the fourth moment theorem, the terms can be simplified as

$$\mathbb{E}\{\mathbf{P}(i)\mathbb{E}\{\mathbf{u}_p(i)\boldsymbol{u}_p{}^T(i)\tilde{\boldsymbol{f}}(i)\tilde{\boldsymbol{f}}^\mathrm{T}(i)\boldsymbol{u}_p(i)\boldsymbol{u}_p{}^T(i)\}\mathbf{P}(i)\}$$

$$= \mathbb{E}\left\{\mathbf{P}(i)\left(2\sigma^4_{\boldsymbol{u}_p}\boldsymbol{K}(i) + \sigma^4_{\mathbf{u}_p}Tr\big(\boldsymbol{K}(i)\big)\right)\mathbf{P}(i)\right\} \qquad (29)$$

Where we represent $\mathbf{K}(i) = \tilde{\boldsymbol{f}}(i)\tilde{\boldsymbol{f}}^T(\mathrm{i})$. Thus, by extracting the diagonal elements, we derive at the following vector recursion:

$$\mathbb{E}\{s(i+1)\} \approx \mathbb{E}\{s(i)\} - 2\mu\mathbb{E}\{\mathbf{P}(i)\}\mathbb{E}\{s(i)\} + \mu^2(2\mathbb{E}\{\boldsymbol{P}^2(i)\}\mathbb{E}\{s(i)\} + \mathbb{E}\{p^2(i)\}\mathbb{E}\{\mathbb{I}^T\, s(i)\}) + \mu^2\frac{\sigma_{\mathbf{v}_p}^2}{\sigma_{\boldsymbol{u}_p}^2}\mathbb{E}\{p^2(i)\} \quad (30)$$

Bound of Learning Rate

When we neglect the inter-dependence of $p_l(i)$ and $\tilde{\boldsymbol{f}}_{\boldsymbol{l}}(i)$ in relation 18, the step-size of $\rho(I - \mu E\{\mathbf{P}(i)\}) < 1$ can make the algorithm converge. The terms of the equations $\mathbf{P}(i)$ is positive definite and $\mathrm{Tr}(\mathbf{P}(i)) = 1$ apart from the fact that we have defined the segments $0 \le g_1(i) \le g_2(i)$. This implies $0 < \mu$ and $\mu < 2/g_2(i)$. Practically, if a gain $g_l(i)$ greater than L^{-1}, the algorithm gives higher convergence rates to some of bigger taps, and on the other hand reduces the convergence speeds of smaller ones.

Steady State Mean Square Deviation

We can calculate the mean square deviation of the proposed algorithms using:

$$MSD = \lim_{i\to\infty}\|E\{s(i)\}\|_1 \approx \frac{\mu\frac{\sigma_{\mathbf{v}_p}^2}{\sigma_{\boldsymbol{u}_p}^2}\sum_{l=1}^{L}\frac{E\{p_l^2(\infty)\}}{E\{p_l(\infty)\}-\mu E\{p_l^2(\infty)\}}}{2-\mu\sum_{l=1}^{L}\frac{E\{p_l^2(\infty)\}}{E\{p_l(\infty)\}-\mu E\{p_l^2(\infty)\}}} \quad (31)$$

For $\mu \ll 1$ the equation for MSD can be simplified into

$$MSD \approx \frac{\mu}{2}\frac{\sigma_{\mathbf{v}_p}^2}{\sigma_{\boldsymbol{u}_p}^2}\sum_{l=1}^{L}\frac{E\{p_l^2(\infty)\}}{E\{p_l(\infty)\}} \quad (32)$$

We know that $E\{x^2\} \ge E^2\{x\}$ for any random variable x. Thus, we come to the conclusion that

$$MSD \ge \frac{\mu}{2}\frac{\sigma_{\mathbf{v}_p}^2}{\sigma_{\boldsymbol{u}_p}^2}\sum E\{p_l(\infty)\} = \frac{\mu}{2}\frac{\sigma_{\mathbf{v}_p}^2}{\sigma_{\mathbf{u}_p}^2} \quad (33)$$

under the constraint of $\mu \ll 1$. We infer from these set of observations that PNLMS algorithm can provide greater steady-state MSD as compared to NLMS algorithm with the same values of μ. $\lambda(i)$ tends to reach zero at steady state; if we have small μ in PEMABPNLMS-II algorithm, we will observe $\zeta < |w_l(i)|$ and $g_l \approx L^{-1}$for majority of blocks. For this case in consideration, the algorithm will tend to attain a similar steady-state MSD value as that of NLMS algorithm.

Time Complexity Analysis

The time complexity for calculations per iteration have been recorded in this section. Describing the NLMS algorithm, L multiplications are made for the feedback path output, 1 for estimating forward path output and $2L + 1$ are used for iterative update of the filter weights. Hence, total of $3L + 2$ multiplications per sample becomes the $\times/\div$ complexity. The $+/-$ complexity is composed of L calculations for feedback tap canceller, 1 for calculating error and L for adaptive weight update. PEM AFC adds a $\times/\div$ complexity of $2K$, K representing the length of PEM filter. Thus, PEMNLMS algorithm's complexity can be estimated. The IPNLMS algorithm uses $5L + 2$ and $4L + 1$ multiplications and additions respectively per iteration. The time complexities of the proposed algorithms are alongside calculated and mentioned in the following table. An example for multiplication complexity has been mentioned for all the algorithms taking $L = 100$ and $K = 21$ and $M = 20$ i.e. taking $P = 5$ for the case and taking estimate of $|N_1(i)| = 50$.

Table 3: Comparison of Computational Complexity per Iteration

Algorithm	$\times/\div$	$+/-$	**Example ($\times$)**	**Example ($+$)**
NLMS	$3L + 2$	$3L + 1$	302	301
PEM NLMS	$3L + 2 + 2K$	$3L + 1 + 2K$	344	343
PEM IPNLMS	$5L + 2 + 2K$	$5L + 1 + 2K$	544	543
PEMABPNLMS - I	$5L + M + 2K + 8$	$5L + M + 2 + 2K$	570	564
PEMABPNLMS- II	$4L + 2K + 17$	$4L + \|N_1(i)\| + 7 + 2K$	459	499

CHAPTER 4

SIMULATION STUDY

The two algorithms which are proposed in the above sections are compared with a set of existing approaches. We have utilized MSG, Added Stable Gain (ASG) and Misalignment (MIS) as the comparison parameters for the performances of all the algorithms. The MIS parameter is defined as the difference of estimated feedback path from that of the actual feedback path in the frequency domain and is denoted using:

$$MIS = 10\,log_{10}\left(\frac{\sum_{i=0}^{N_f-1}|H(e^{j\omega_i})-W(e^{j\omega_i})|^2}{\sum_{i=0}^{N_f-1}|H(e^{j\omega_i})|^2}\right) \quad (34)$$

where the count of the frequency samples used is represented by N_f. The parameter Maximum Stable Gain (MSG) is computed at the frequency which maximizes the difference between true and estimated feedback path.

$$MSG = 20\,log_{10}\left(\min_{w}\frac{1}{|H(e^{j\omega_i})-W(e^{j\omega_i})|}\right) \quad (35)$$

Lastly, Additional gain which can be added to the system under effective acoustic feedback cancellation maintaining the stability is defined as ASG.

$$ASG = MSG - 20\,log_{10}\left(\min_{w}\frac{1}{|H(e^{j\omega_i})|}\right) \quad (36)$$

Indications of a higher modeling accuracy is provided by smaller MIS values, which signifies improved feedback cancellation. Moreover, a higher Additional gain values correspond to feedback cancellation mechanisms which provide higher ranges for stable operations under stable and satisfactory feedback cancellation.

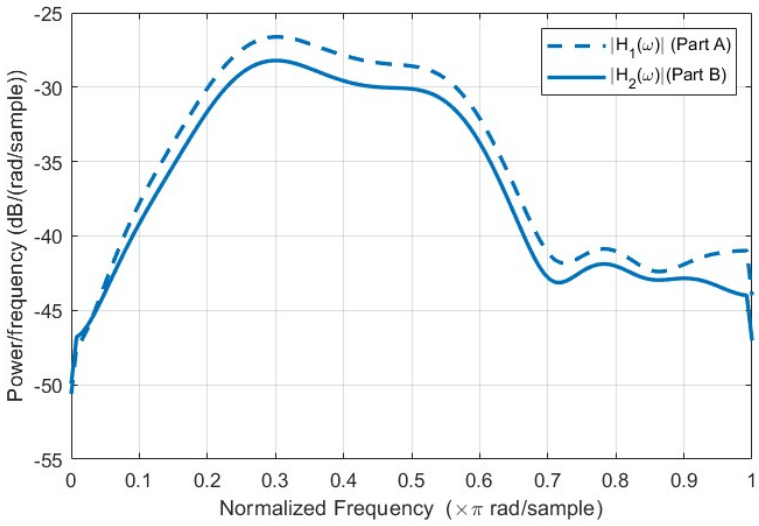

Figure 3: Power Spectral Density of the Acoustic Feedback paths

The effectiveness of the proposed methodologies can be measured using other parameters such as PESQ (Perceptual Evaluation of Speech Quality). The value of the parameter varies from 0.5 to 4.5, with higher value representing higher excellence. On the other hand, PEAQ, or Perceptual Evaluation of Audio Quality, can be implemented for evaluating audio signal's quality to compare original signal with the output signal. It gives a score in the range of 0 (no perceivable impairment) to -4 (highly terrible impairment).

The intelligibility index used for our work includes HASQI and HAAQI. They both process and compare the input and degraded outputs over the model of the auditory periphery for normal and impaired hearing. The comparison is done once the signals are aligned with each other. The Hearing Aids Speech Quality Index computes the cochlear outputs for a reference signal to the output. The metric is particularly responsive to shifts in the speech spectrum resulting from acoustic feedback or whistling in the hearing aid (HA), as well as to any nonlinear distortion caused from the feedback cancellation process.

Case I: Speech Input Without Path Tracking

For the first case at simulations study, we have used a 25khz sample frequency speech input down sampled at 16kHz which can be seen in Figure 4. (a). The acoustic feedback path has 100 coefficients. The forward Gain of the system has a transfer function $F(z) = 8z^{-48}$, implying a delay of 3ms. There are plots Figure 4. (b) MIS, Figure 4. (c) ASG and Figure 4. (d) MSG which provides evidence for higher levels of added stable gain and better convergence for proposed algorithms. **T**he parameters for all the algorithms discussed are as follows: $\mu = 0.002$ for NLMS with $\epsilon = 1e^{-5}$; PEM NLMS $\epsilon = 1e^{-5}$; $\alpha = 0.5$ for PEMIPNLMS with $\epsilon = 1e^{-5}$. For the proposed algorithm PEMABPNLMS-I the parameters are P = 5, $\epsilon = 1e^{-5}$,$\gamma = 0.95$, while that for PEMABPNLMS-II the parameters are set to $\epsilon = 1e^{-5}$, $\beta = 0.98$, $\gamma = 0.99$, $\kappa = 0.3$, $\gamma_1 = 0.97$. The Perceptual Evaluation of Speech Quality (PESQ) score has been calculated using the last 10 seconds i.e. last 1,60,000 samples for both loudspeaker output and error signal.

Table 4: PESQ and HASQI Score for Speech signal without path tracking.

Algorithm	**PESQ Score**	**HASQI Score**
NLMS	3.4347	0.9989
PEM NLMS	3.9334	0.9965
PEM IPNLMS	4.3040	0.9956
PEM ABPNLMS – I	4.3806	0.9957
PEM ABPNLMS – II	4.2150	0.9999

Case II: Speech Input with Path Tracking

There can be various reasons for acoustic path change while speech source still providing signal. The acoustic feedback path for the system may thus change and it becomes a feature of the acoustic feedback cancellation algorithm to retrack the acoustic path to re estimate it. The magnitude response for both the paths are plotted in Figure 3.

The input is taken as same described in CASE-I. The forward path transfer function $F(z) = 10z^{-48}$. The plots are plotted and the corresponding parameters description for algorithms are as follows:$\mu = 0.002$ for NLMS with $\epsilon = 1e^{-5}$; PEM NLMS $\epsilon = 1e^{-3}$; $\alpha = 0.5$ for PEMIPNLMS with $\epsilon = 1e^{-5}$. For the proposed algorithm PEMABPNLMS-I the parameters are P = 5, $\epsilon = 1e^{-5}$,$\gamma = 0.95$, while that for PEMABPNLMS-II the parameters are set to $\epsilon = 1e^{-5}$, $\beta = 0.98$, $\gamma = 0.99$, $\kappa = 0.3$, $\gamma_1 = 0.97$. The Perceptual Evaluation of Speech Quality (PESQ) score has been calculated using the last 10 seconds i.e. last 1,60,000 samples for both loudspeaker output and error signal.

Table 5: PESQ Score for observed change in acoustic path - Path Tracking in case of speech input

Algorithm	**PESQ Score before path change**	**PESQ Score after path change**
NLMS	3.3888	2.7036
PEM NLMS	4.2335	3.8185
PEM IPNLMS	4.3386	4.0509
PEM ABPNLMS – I	4.3713	4.1222
PEM ABPNLMS – II	4.3885	4.1735

Table 6: HASQI Score for observed change in acoustic path for speech input.

Algorithm	**HASQI Score before path change**	**HASQI Score after path change**
NLMS	0.9971	0.9991
PEM NLMS	0.9988	0.9989
PEM IPNLMS	0.9958	0.9990
PEM ABPNLMS – I	0.9963	0.9990
PEM ABPNLMS – II	0.9963	0.9990

Case III: Audio Input with Path Tracking

Music audio input sample (Figure 6. (a)) for analyzing the performance measures are taken from LABROSA with the sampling frequency of 16kHz. The forward path gain is set to 15, for which the plots are given in Figure 6. The simulation parameters are: $\mu = 0.003$ for NLMS with $\epsilon = 1e^{-5}$; PEM NLMS $\epsilon = 1e^{-3}$; $\alpha = 0.5$ for PEMIPNLMS with $\epsilon = 1e^{-5}$. For the proposed algorithm PEMABPNLMS-I the parameters are P = 5, $\epsilon = 1e^{-5}$, $\gamma = 0.9$, while that for PEMABPNLMS-II the parameters are set to $\epsilon = 1e^{-5}$, $\beta = 0.98$, $\gamma = 0.95$, $\kappa = 0.3$, $\gamma_1 = 0.97$. The Perceptual Evaluation of Speech Quality (PESQ) score has been calculated using the last 10 seconds i.e. last 1,60,000 samples for both loudspeaker output and error signal.

Table 7: PEAQ Score for observed change in acoustic path - Path Tracking in case of speech input

Algorithm	**PEAQ Score before path change**	**PEAQ Score after path change**
NLMS	-2.721	-3.503
PEM NLMS	-2.588	-2.170
PEM IPNLMS	-2.359	-2.212
PEM ABPNLMS – I	-2.219	-2.314
PEM ABPNLMS – II	-2.351	-2.030

Table 8 : HAAQI Score for observed change in acoustic path.

Algorithm	**HAAQI Score before path change**	**HAAQI Score after path change**
NLMS	0.9880	0.9677
PEM NLMS	0.9889	0.9794
PEM IPNLMS	0.9922	0.9832
PEM ABPNLMS – I	0.9965	0.9854
PEM ABPNLMS – II	0.9928	0.9982

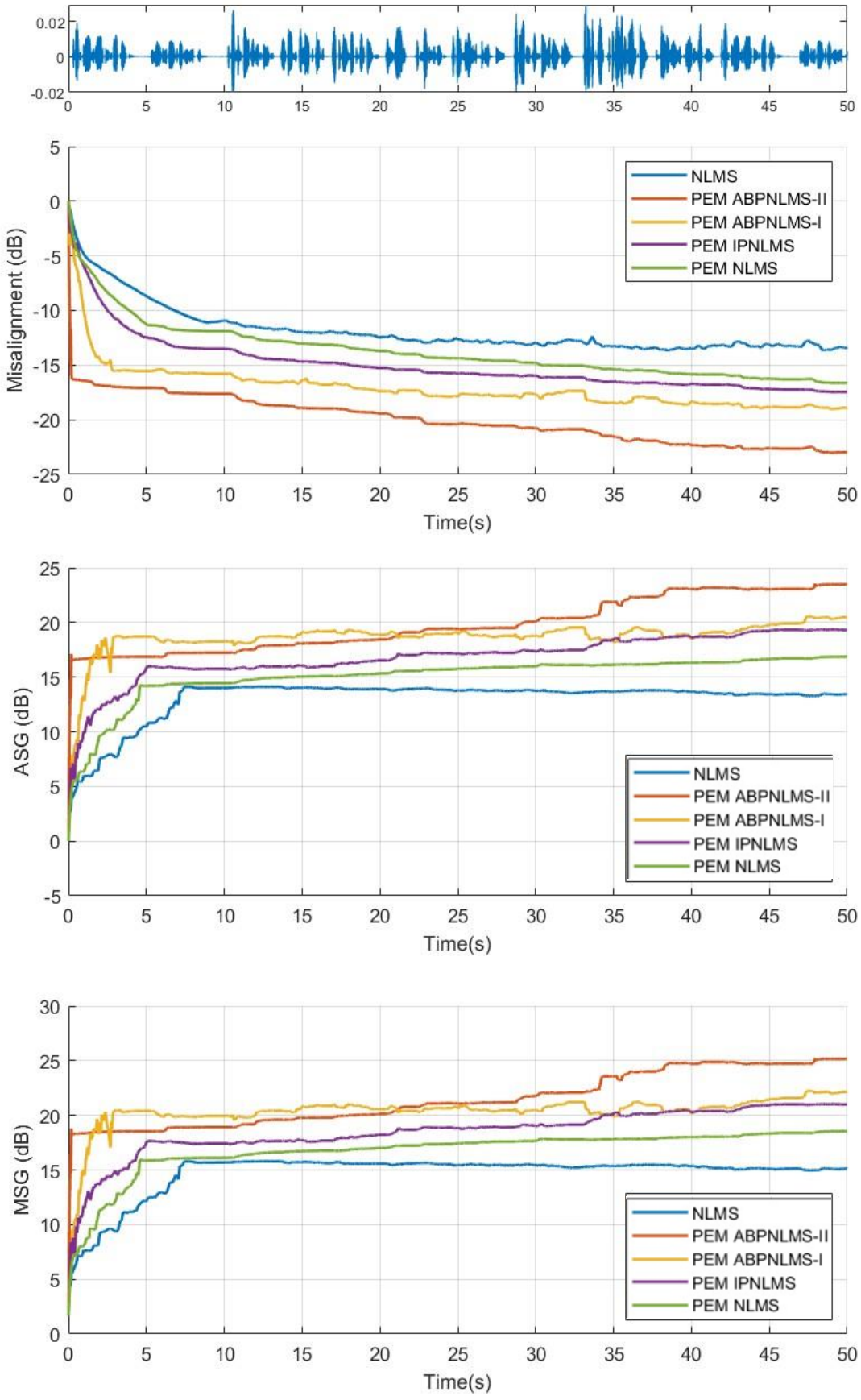

Figure 4:(a) Speech input signal and corresponding (b) MIS (c) ASG (d) MSG plots for acoustic feedback cancellation in Hearing aids

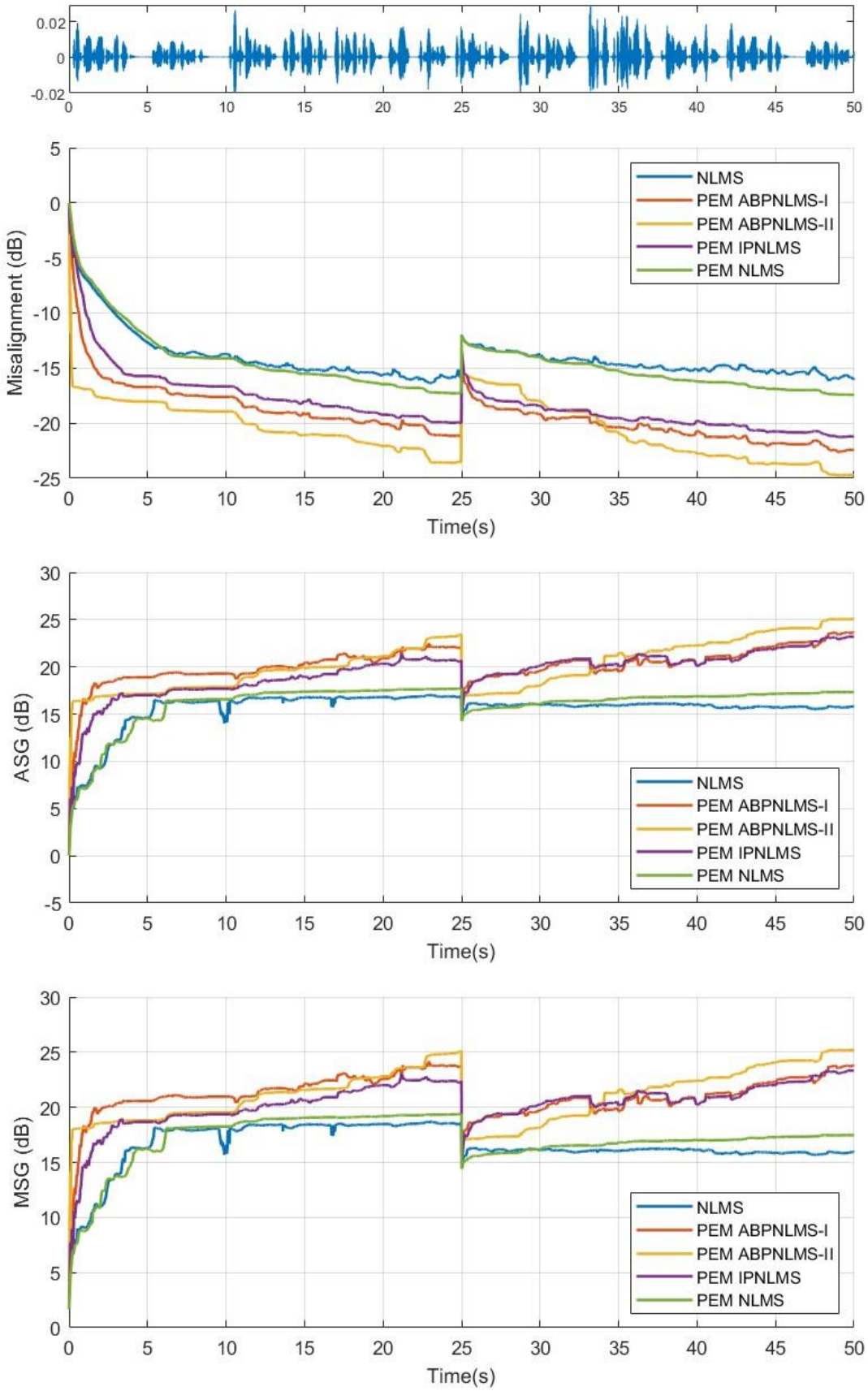

Figure 5(a) Speech input signal and corresponding (b) MIS (c) ASG (d) MSG plots for acoustic feedback cancellation in Hearing aids for path tracking

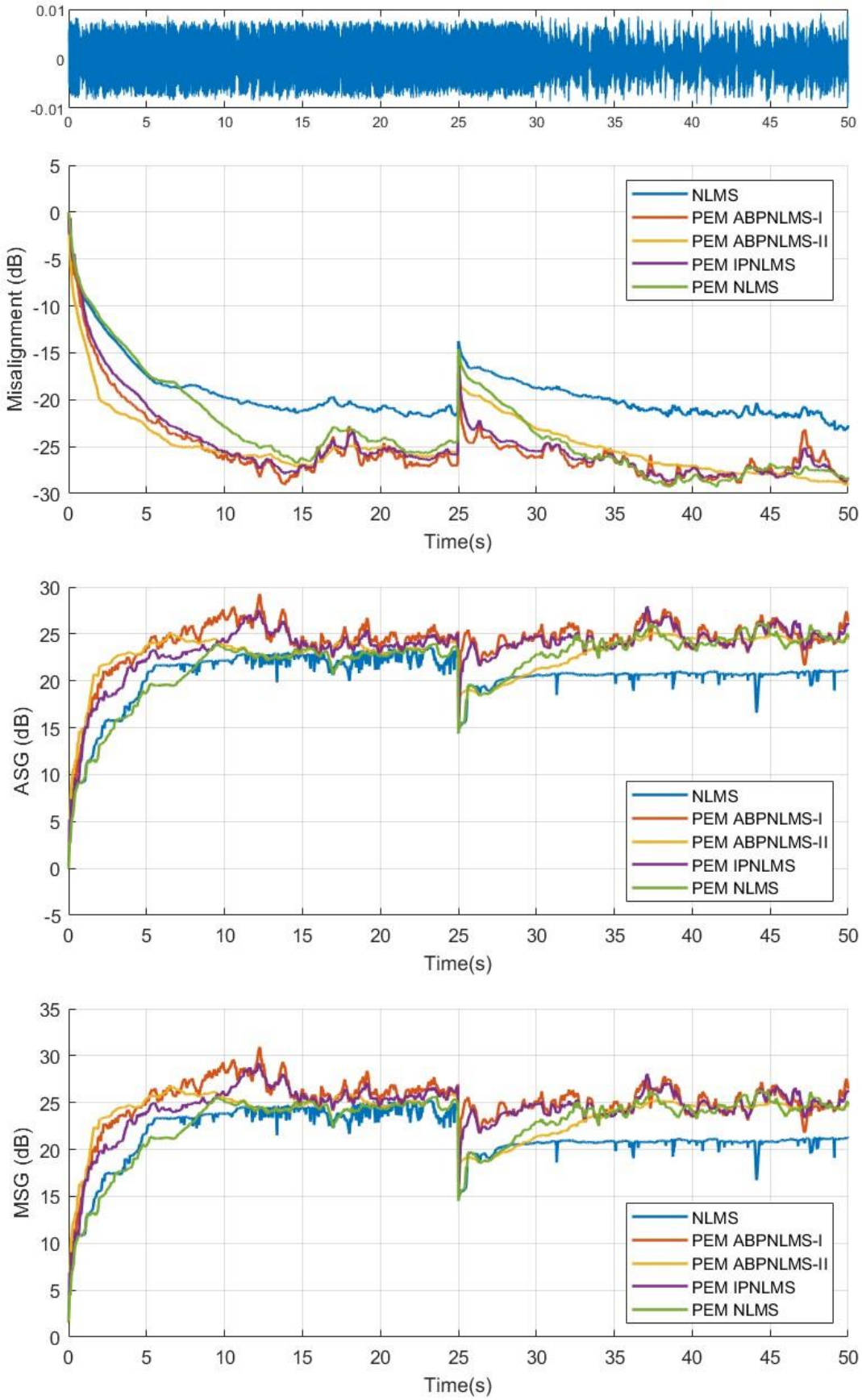

Figure 6(a) Audio input signal and corresponding (b) MIS (c) ASG (d) MSG plots for acoustic feedback cancellation in Hearing aids for path tracking

CHAPTER 5

CONCLUSION AND FUTURE SCOPE

In this paper two novel approaches for sparse systems towards achieving improved MIS convergence levels and Added gain for hearing aids have been proposed. An online estimate for input signal power has been implemented for providing realistic HA implementation. We have used a variety of HA matrices to compare the algorithms performance with others including HASQI and HAAQI along with PESQ and PEAQ. The two algorithms achieve significant good performance under greater step-sizes, unlike NLMS and IPNLMS, which leads to the applicability of algorithms for severe hearing impairment. This also suggests that we can further make the algorithm attain better convergence if integrated with VSS or improved versions for practical implications. Merging the algorithm with PEM increases the efficiency of the algorithm to a further extent. Exploring optimal dynamic non-uniform partition methods for development of modified versions of algorithm for non-sparse systems can be a related field of study for enthusiasts.

REFERENCES

[1] G. Rombouts, T. van Waterschoot, K. Struyve and M. Moonen, "Acoustic feedback cancellation for long acoustic paths using a nonstationary source model," in IEEE Transactions on Signal Processing, vol. 54, no. 9, pp. 3426-3434, Sept. 2006, doi: 10.1109/TSP.2006.879251.

[2] Chengshi Zheng, Meihuang Wang, Xiaodong Li, Brian C. J. Moore; A deep learning solution to the marginal stability problems of acoustic feedback systems for hearing aids. *J. Acoust. Soc. Am.* 1 December 2022; 152 (6): 3616–3634. https://doi.org/10.1121/10.0016589

[3] Chung K. Challenges and Recent Developments in Hearing Aids: Part II. Feedback and Occlusion Effect Reduction Strategies, Laser Shell Manufacturing Processes, and Other Signal Processing Technologies. Trends in Amplification. 2004;8(4):125-164. doi:10.1177/108471380400800402

[4] Jyoti Maheshwari, Nithin V. George, Robust modeling of acoustic paths using a sparse adaptive algorithm, Applied Acoustics, Volume 101, 2016,Pages 122-126, ISSN 0003-682X, https://doi.org/10.1016/j.apacoust.2015.08.013.

[5] Christos Boukis, Danilo P. Mandic, Anthony G. Constantinides; Toward bias minimization in acoustic feedback cancellation systems. *J. Acoust. Soc. Am.* 1 March 2007; 121 (3): 1529–1537. https://doi.org/10.1121/1.2431341

[6] S. Laugesen, K. V. Hansen, J. Hellgren; Acceptable delays in hearing aids and implications for feedback cancellation. *J. Acoust. Soc. Am.* 1 February 1999; 105 (2_Supplement): 1211–1212. https://doi.org/10.1121/1.425698

[7] M. G. Siqueira and A. Alwan, "Steady-state analysis of continuous adaptation in acoustic feedback reduction systems for hearing-aids," in IEEE Transactions on Speech and Audio Processing, vol. 8, no. 4, pp. 443-453, July 2000, doi: 10.1109/89.848225.

[8] S. Pradhan, X. Qiu and J. Ji, "A Variable Step Size Improved Multiband-Structured Subband Adaptive Feedback Cancellation Scheme for Hearing Aids," 2020 Asia-Pacific Signal and Information Processing Association Annual Summit and Conference (APSIPA ASC), Auckland, New Zealand, 2020, pp. 681-685.

[9] F. Albu, L. Tran, S. Radhika and A. Chandrasekar, "Acoustic Feedback Cancellation using the Variable Step Size Affine Projection Tanh Algorithm," 2023 IEEE Statistical Signal Processing Workshop (SSP), Hanoi, Vietnam, 2023, pp. 522-526, doi: 10.1109/SSP53291.2023.10208063.

[10] Parth Mishra, Serkan Tokgoz, Issa M. S. Panahi; Robust real-time implementation of adaptive feedback cancellation using noise injection algorithm on smartphone. *Proc. Mtgs. Acoust.* 7 May 2018; 33 (1): 055003. https://doi.org/10.1121/2.0000836

[11] (springer article) Eren, Y., Güvenç, B.Ç. & Mengüç, E.C. An acoustic feedback canceler based on probe noise and informative data for hearing aids. SIViP 18, 703–714 (2024). https://doi.org/10.1007/s11760-023-02786-7

[12] Sankha Subhra Bhattacharjee, Nithin V. George, Fast and efficient acoustic feedback cancellation based on low rank approximation, Signal Processing, Volume 182,2021,107984,ISSN 0165 1684, https://doi.org/10.1016/j.sigpro.2021.107984.

[13] Siva Prasad, S., & Rama Rao, C. (2022). Optimal Step Size Technique for Frequency Domain and Partition Block Adaptive Filters for PEM based Acoustic Feedback Cancellation. *Defence Science Journal*, *72*(5), 742-752. https://doi.org/10.14429/dsj.72.17881

[14] J. Liu, Q. Liu, W. Wang and X. -. L. Wang, "An Improved MLMS Algorithm with Prediction Error Method for Adaptive Feedback Cancellation," *2021 International Conference on Security, Pattern Analysis, and Cybernetics （SPAC)*, Chengdu, China, 2021, pp. 397-401, doi: 10.1109/SPAC53836.2021.9539993.

[15] R Vanitha Devi, Vasundhara, Curvelet based robust improved sine adaptive filter for feedback cancellation in hearing aids, Applied Acoustics, Volume 211, 2023,109528,ISSN 0003-682X, https://doi.org/10.1016/j.apacoust.2023.109528.

[16] Tran LTT, Nordholm SE. A Switched Algorithm for Adaptive Feedback Cancellation Using Pre-Filters in Hearing Aids. *Audiology Research*. 2021; 11(3):389-409. https://doi.org/10.3390/audiolres11030037

[17] Sven Nordholm, Henning Schepker, Linh T. T. Tran, Simon Doclo; Stability-controlled hybrid adaptive feedback cancellation scheme for hearing aids. *J. Acoust. Soc. Am.* 1 January 2018; 143 (1): 150–166. https://doi.org/10.1121/1.5020269

[18] R Vanitha Devi, Vasundhara, Curvelet based robust improved sine adaptive filter for feedback cancellation in hearing aids, Applied Acoustics, https://doi.org/10.1016/j.apacoust.2023.109528

[19] Pradhan, S.; Patel, V.; Patel, K.; Maheshwari, J.; George, N.V. Acoustic feedback cancellation in digital hearing aids: A sparse adaptive filtering approach. *Appl. Acoust.* **2017**, *122*, 138–145.

[20] L. T. T. Tran, S. E. Nordholm, H. Schepker, H. H. Dam and S. Doclo, "Two-Microphone Hearing Aids Using Prediction Error Method for Adaptive Feedback Control," in IEEE/ACM Transactions on Audio, Speech, and Language Processing, vol. 26, no. 5, pp. 909-923, May 2018, doi: 10.1109/TASLP.2018.2798822.

[21] M. T. Akhtar, F. Albu and A. Nishihara, "Prediction Error Method (PEM)-Based Howling Cancellation in Hearing Aids: Can We Do Better?," in IEEE Access, vol. 11, pp. 337-364, 2023, doi: 10.1109/ACCESS.2022.3232334.

[22] Y. Chen, Y. Gu and A. O. Hero, "Sparse LMS for system identification", Proc. IEEE ICASSP, pp. 3125-3128, Apr. 2009.

[23] Y. Gu, J. Jin and S. Mei, "\$ell _{0}\$ norm constraint LMS algorithm for sparse system identification ", IEEE Signal Process. Lett., vol. 16, no. 9, pp. 774-777, Sep. 2009.

[24] J. Meng et al., " A reweighted \$ell _{0}\$ -norm-constraint LMS algorithm for sparse system identification ", Digit. Signal Process., vol. 123, Apr. 2022.

[25] S. Jiang and Y. Gu, "Block-sparsity-induced adaptive filter for multi-clustering system identification", IEEE Trans. Signal Process., vol. 63, no. 20, pp. 5318-5330, Oct. 2015.

[26] W. Wang and H. Zhao, " A novel block-sparse proportionate NLMS algorithm based on the \$ell _{20}\$ norm ", Signal Process., vol. 176, Nov. 2020.

[27] F. Strasser and H. Puder, "Adaptive Feedback Cancellation for Realistic Hearing Aid Applications," in IEEE/ACM Transactions on Audio, Speech, and Language Processing, vol. 23, no. 12, pp. 2322-2333, Dec. 2015, doi: 10.1109/TASLP.2015.2479038.

[28] E. V. Kuhn, F. d. C. de Souza, R. Seara and D. R. Morgan, "On the Steady-State Analysis of PNLMS-Type Algorithms for Correlated Gaussian Input Data," in IEEE Signal Processing Letters, vol. 21, no. 11, pp. 1433-1437, Nov. 2014, doi: 10.1109/LSP.2014.2332751.